

# FE-MODELLING GUIDELINES FOR THE DIMENSIONING OF AIRCRAFT CABIN INTERIOR UNDER STATIONARY DYNAMIC LOADS

**R. Seemann\*, B. Plaumann\*, J. Oltmann\*, D. Krause\***  
\* Hamburg University of Technology (TUHH),

**Keywords: sustained engine imbalance, cabin interior, FE-modelling**

## Abstract

*Cabin interior monuments are usually substantiated by worst case quasi-static testing validation supported by simplified FE-computation for determining the static interface loads and global deflection. With the increasing relevance of stationary dynamic loads, for instance due to sustained engine imbalance, the question arises whether the currently used FE-models are still sufficient for such load cases. The present contribution shows benchmark test data and modelling studies for dynamic loading.*

## 1 Introduction

Due to FAA and EASA requirements for the structural substantiation of aircraft cabin interior monuments, the dimensioning of cabin interior has been largely relying on worst-case validation using quasi-static tests along with static FE-simulations for the prediction of the interface loads between monument and primary aircraft structure as well as the maximum deflection. However, with the announcement of the re-engined single aisle aircraft programs of both large OEMs, stationary dynamic loading resulting from the so called “sustained engine imbalance” (SEI) condition receives increasing attention from aircraft cabin structural engineers. This condition is also known as “windmilling” and results from fan blade-loss in the engine, for instance due to foreign object damage or fatigue failure as in Fig. 1. In this event, the engine is usually cut-off while the air flow of the aircraft in flight keeps the engine rotating. The ambient imbalance of the broken fan blade causes a stationary vibrational excitation of considerable magnitude which is

transmitted through the entire aircraft including the cabin [1]. Since braking the engine would lead to a tremendous increase in drag, it is desirable to tolerate this windmilling condition. Yet the substantiation of all affected components is recommended by the aviation authorities (FAR25 [3] and CS25 [4]). The frequency of such an event can be estimated based on an extensive analysis of the service history of blade loss windmilling events between 1972-1997 [6]. This report suggests that the likelihood of a 1h diversion mission is  $10^7 - 10^8$  per flight hour and  $10^9$  per flight hour for a 3h diversion mission. Considering data of total commercial flight hours as given for instance by the US Bureau of Transportation Statistics [7], this would indicate a few events per year if the projected rate of [6] is still applicable.



Fig. 1: Fan blade loss from fatigue failure (courtesy of ATSB, investigation number 200100445) [5]

The re-engined single aisle aircraft programs are driven by the implementation of new fuel-efficient high-bypass turbofan engines, whereas changes to the remaining aircraft are limited. In case of SEI, the considerably larger fan of these engines inevitably leads to a higher energy transmission into the aircraft structure, if compared to the A320 legacy program. As a

consequence, there is some uncertainty with regards to the structural behavior of cabin interior monuments under SEI loads when considering the re-engined aircraft. Due to the interface between cabin monuments and aircraft primary structure, this uncertainty concerns not only the cabin interior supplier but also the structural engineers of the aircraft OEMs. Considering that the excitation frequencies of the SEI condition lie in the range of the resonance frequency of the cabin monuments and the vicinity of the passengers to the monuments, this condition is clearly safety critical and has to be addressed carefully.

The present work gives an overview on how the described stationary dynamic loads can be considered in a linear finite element model of cabin interior monuments. Proprietary test data from comprehensive full scale tests of cabin monuments under windmilling loads serve as a benchmark.

## 2 FE-Simulation of Cabin Interior Under Quasi-Static Loading

The aircraft cabin industry is still somewhat lagging behind with regards to the concurrent application of FE-Simulation during the product design phase if compared to other aircraft related industries [2]. Currently, FE-computation is mainly used to complement the substantiation process at the end of the design phase, by supplying adequate interface loads (IFL) and deflection of the cabin structures. These linear-static global analyses are usually based on rather crude FE-models, which apply two dimensional shell elements to represent the honeycomb sandwich panels with either homogenized material properties or discrete-layer property sets where the panels are divided into three or more layers. Typical element sizes for such models range between 50-150mm. Interfaces and joints are usually significantly simplified, with panel-to-panel joints often represented by merged nodes at the edges. The actual supporting structure of the monuments in the aircraft is represented by discrete spring elements with stiffness values as given by the OEMs [8]. The upper tie rods are implemented using rod elements. Additional components, such as ovens, standard units or literature

pockets are reduced to lumped masses, which are attached to the shell structure via interpolation constraint elements. Reinforcements like aluminum fittings or linings are sometimes modelled using 1D or solid elements. Figure 1 displays a typical FE-model of an aircraft galley intended for the computation of the interface loads resulting from static load cases.

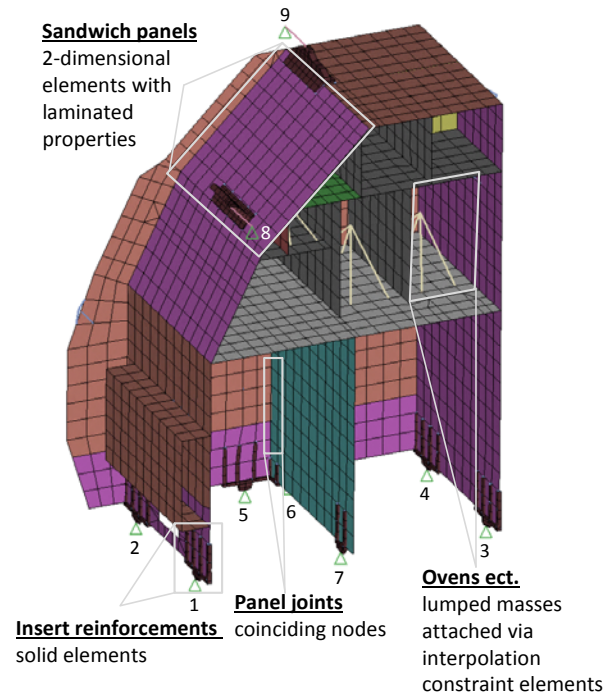


Fig. 2: Galley - FE-model with hardpoint and tie rod connections 1-9

## 3 Experimental Studies of Cabin Interior Under Stationary Dynamic Loading

Testing structures under stationary dynamic loads is usually done on custom design hydraulic test rigs which allow periodic one-axial linear motions at a given frequency and acceleration. At the institute PKT various windmilling excitation tests with cabin monuments have been performed using an elaborate 6-dof test rig (Fig. 3). This hexapod test rig has been funded by the DFG (German Research Foundation) and is capable of exciting large structures of up to 1.5 tons beyond 1.3g at frequencies of up to 30 Hz. The innovative iterative control system of the facility maintains excellent signal quality based on non-linear system identification algorithms. The static

capabilities of the test rig range up to 500kN and 40kNm with a positioning range of +/-300 mm. The design with 6 independent degrees of freedom has the benefit that the investigated structure can be tested in all translatory directions without changing the test setup, while arbitrary multi-axial excitations can be applied as well.

### 3.1 Test Description

The A320 G2 Galley provided by our cooperation partner Diehl Service Modules was mounted onto the hexapod as shown in Fig. 2, using a rigid floor structure as well as a rigid aluminum backframe without fixture resonances in the excitation frequency band for the upper attachments. The galley was attached to the floor structure at its 6 hardpoints and 1 flutter point. The 2 upper tie rod attachments were connected to the aluminum backframe. 3D load cells were positioned at the 7 lower attachments and 1d load cells were inserted at the tie rod connection. The measurement for fully loaded condition did not include a force measurement at the trolley wheels. Therefore the load path shortcut through the trolley wheels is not measured.



Fig. 3. Fully loaded G2 on the hexapod test rig [12]

The tests were conducted with four different loading conditions, namely empty, fixed-only, without trolleys and fully loaded. The definition of the loading condition is summarized in Tab.1. The system identification tests have been run with swept sine excitations between 3 and 25Hz with a frequency ascend of

0.5 octaves per minute at three different constant acceleration levels (0.5g, 1g and 1.3g). In order to increase the weight of all galley inserts and compartments to the allowed maximum weight, dummy loadings of 0.5l PET water bottles and packs of 500 paper sheets have been applied. This loading is assumed to resemble actual in-flight situations.

Tab.1. Tested loading condition of the G2 Galley

loading condition	empty	fixed only	w/o trolley	full
ovens		X	X	X
beverage maker		X	X	X
standard Units			X	X
compartments			X	X
trolleys				X
add-on loading [kg]	0	96	166	416
gross weight [kg]	135	231	301	551

Due to fine dust emission from crushed insulation of real ovens in previous tests, wooden oven dummies from static substantiation tests at Diehl Service Modules were used instead of real ovens.



Fig. 4: Loading substitutes for trolley testing

### 3.2 Test Evaluation

#### 3.2.1 Damping, Forces, Acceleration

In the following description of the dynamic galley behavior, the measure of acceleration transmissibility has been used as a benchmark for the comparison of simulation and test data. The only global mode within the considered frequency range is evident under excitation in Y-direction. Therefore, an acceleration transmissibility of the common Y-excitation, equal at all interfaces, to the point of maximum Y-deflection (response) in the global mode is used as depicted in Fig. 4.

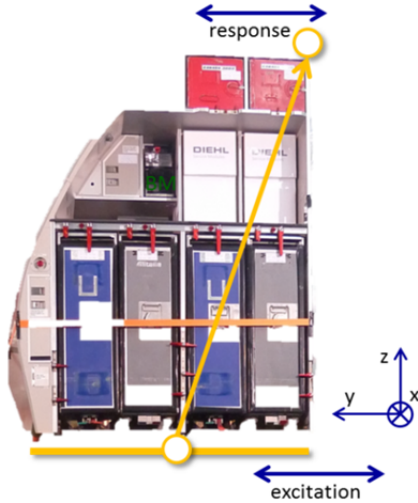


Fig. 5. Acceleration transmissibility considered as benchmark description of the global dyn. behavior [13]

The acceleration transmissibility is therefore defined as

$$F(\omega) = \frac{a_{out}}{a_{exc}} \quad (1)$$

with the input acceleration  $a_{exc}$  and the output acceleration  $a_{out}$  at the point of maximum deflection in the global mode.

Tab. 2. Acceleration transmissibility from excitation to the highest global mode deflection (Y-excitation)

loading condition		empty	fixed only	w/o trolley	full
<b>0.5g</b>	<b>Y</b>				
	<b>frequency</b> [Hz]	21	16	16	15
	<b>trans-</b> <b>missibility</b>	28	5.1	3.4	2.9
<b>1.0g</b>	<b>Y</b>				
	<b>frequency</b> [Hz]	20	17	18	19
	<b>trans-</b> <b>missibility</b>	15	5.6	3.5	3.5
<b>1.3g</b>	<b>Y</b>				
	<b>frequency</b> [Hz]	-	17	16	17
	<b>trans-</b> <b>missibility</b>	-	4.3	3.5	3.5

Tab. 2 shows the acceleration transmissibility in the first global mode from the excitation acceleration at the fixation to the maximum deflection point in the global mode at the front right upper corner of the galley.

A clearly non-linear behavior regarding the excitation level can be noted. Interestingly, the vibration behavior gets less significant with higher loading. The highest interface loads were

measured for the empty galley with interface forces gradually reducing with higher loading. This may contradict a first guess estimation based on mass, but it originates from the significantly higher damping contribution of the sliding masses of loading in the containers, trolleys and ovens.

### 3.2.2 Dynamic Mass Analysis

In order to obtain an understanding of relevant characteristics of the dynamic behavior of the tested galley, a dynamic mass analysis has been performed. For this, the frequency response function of the resulting interface forces (summed up in each translatory direction) over the excitation acceleration has been computed in a comparative study for all loading conditions. This first analysis focusses on the global dynamic behavior of the galley and tries to identify local influences. Modelling the vibrational behavior of subcomponents like the galley ovens is covered in the following section 4.2.2.

The global comparison is based on a 1g constant excitation level except for the X-direction fixed-only measurement, where the measurement data was corrupted and the 1.3g case has been used instead. With the dynamic mass FRF of interface load sum, the only global mode can be clearly identified in the Y-direction for all loading conditions. However, a mass decoupling of loose galley inserts or loose sliding masses (dummy loads) within the galley inserts is overlaying. Tab. 3 presents the different loading variations. It can be clearly seen that the trolleys decouple before the sweep reaches 8Hz, both under Y- and X-excitation.

For the w/o trolley condition, it can be seen that the standard units (3x15kg) decouple by a quarter of their mass equivalent (together  $\Delta m=12\text{kg}$ ) when excited in X-direction, but not in Y-direction. This can be explained by the stacking of the water bottles in the standard units with gravity pressing the bottles closely together when lying side-to-side in the Y-direction while in X-direction there is some free room between standard unit walls and bottles. Looking at the overall galley behavior a decoupling of ovens and oven loading mass cannot be identified.

**FE-MODELLING GUIDELINES FOR THE DIMENSIONING OF AIRCRAFT CABIN INTERIOR UNDER STATIONARY DYNAMIC LOADS**

X-excitation	Y-excitation
<p><b>Empty: 135kg gross weight</b> empty galley structure</p> <p><math>m_{dyn}(3Hz) \approx 185kg</math>, no mass decoupling detected, slow increase due to platform tilting or 2nd bending mode above 25Hz</p>	<p><b>Empty: 135kg gross weight</b> empty galley structure</p> <p><math>m_{dyn}(3Hz) \approx 165kg</math>, no mass decoupling detectable</p>
<p><b>Fixed-only: 231kg gross weight</b> two loaded oven dummies and one beverage maker added to empty galley</p> <p><math>m_{dyn}(3Hz) = 280kg</math>, no mass decoupling detectable</p>	<p><b>Fixed-only: 231kg gross weight</b> two loaded oven dummies and one beverage maker added to empty galley</p> <p><math>m_{dyn}(3Hz) = 265kg</math>, no mass decoupling detectable</p>
<p><b>w/o Trolleys: 301kg gross weight</b> three loaded standard units and three loaded compartments added to fixed-only</p> <p><math>m_{dyn}(3Hz) \approx 330kg</math>, <math>m_{dyn}(6Hz) \approx 318kg</math> loaded standard units (all together 45kg) show mass decoupling of 12kg equivalent</p>	<p><b>w/o Trolley: 301kg gross weight</b> three loaded standard units and three loaded compartments added to fixed-only</p> <p><math>m_{dyn}(3Hz) \approx 340kg</math>, <math>m_{dyn}(6Hz) \approx 340kg</math> no mass decoupling detectable</p>
<p><b>Fully loaded: 551kg gross weight</b> 4 trolleys (2x 50kg and 2x 75kg) added to w/o trolley condition</p> <p><math>m_{dyn}(3Hz) \approx 525kg</math> <math>m_{dyn}(8Hz) \approx 330kg</math> <math>m_{dyn}(6Hz) \approx 350kg</math> multiple mass decoupling present of 195kg</p>	<p><b>Fully loaded: 551kg gross weight</b> 4 trolleys (2x 50kg and 2x 75kg) added to w/o trolley condition</p> <p><math>m_{dyn}(3Hz) \approx 640kg</math> <math>m_{dyn}(9Hz) \approx 300kg</math> trolleys show mass decoupling of 340kg mass equivalent</p>

But as shown in a study presented in [9], they do show some directional depended mass decoupling also. It amounts to ca. 10kg mass equivalent per oven, both in X- and Y-direction.

The occurrence of the described decoupling effects shall be one option for the simplified FE-modelling of cabin monuments where the galley inserts are usually represented by lumped masses with their maximum gross weight. This lumped mass approach for galley insert modelling shall be investigated and compared to a modelling of geometrically approximated shell structures.

#### 4 FE-Simulation of Cabin Interior Under Stationary Dynamic Loading

This section aims to describe recommendations on how to develop a validated dynamic model for cabin interior using adequate experimental data. Starting point for the present study is a validated static FE-model which is supposed to be transferred to a dynamic FE-model. The following numerical simulations have been carried out with MSC.Nastran.

It is shown that simple modelling techniques can lead to reasonably accurate models for the dynamic behavior of lightweight honeycomb sandwich structures. However, it should be noted that due to the linear nature of the applied model, no true peak loads resulting from impacting components during vibration can be predicted. For these purposes more sophisticated non-linear models are necessary that include impact behavior. In this paper, the modelling focus is put on early stages in product development. The FE-simulations presented here shall enable reasonable forecasts to support design engineers when dimensioning aircraft monuments. Key design criteria include the resonance frequency and the interface loads.

In the present study, the maximum global acceleration transmissibility serves as a benchmark for comparing simulation and test results. Additionally the highest resulting interface loads (hardpoint no. 4, see Fig. 2) are shown exemplarily for demonstrating a possible prediction with the help of the model. The underlying static model (starting model) is depicted in Fig. 2. It follows the model description as given in section 2. The objective

is to keep the described simplicity of the model while the dynamic behavior resulting from SEI loads can be represented with sufficient accuracy.

#### 4.1 Starting Model

As a first step, the starting model has been subjected to a dynamic sweep excitation instead of the usual quasistatic loads. For the simulation of the galley's resonance behavior, additional masses were not considered. This case is described in Tab. 1 as an 'empty' galley. A sinusoidal acceleration with constant 1g amplitude was applied at all supports over a frequency interval of 3 - 25 Hz (analogous to the experiments).

The mechanical damping behavior of the galley structure has been implemented by overall global structural damping derived from test data (see section 3) and adapted by matching the amplification behavior of simulation and test. The model tuning greatly benefits from the used Hexapod test facility that enables modal parameter estimation of large and heavy test specimens like galleys in complicated multiple input, multiple output (MIMO) tests with a high degree of accuracy, despite its possible complications [11].

For post-processing purposes, the resonance behavior in all 3 translatory excitation directions was reviewed. Not all results, however, show relevant resonance peaks regarding the determination of critical load cases (see e.g. Fig. 5, case Y-Z). Therefore these cases shall be neglected here and the focus is put on excitations in Y-direction.

The resonance frequency of the starting model differs from the test results by ~19% (see Fig. 5). The amplification matches approximately the test results and is just slightly higher. The interface loads, however, underestimate the actual loads in the hardpoint determined by the tests.

#### 4.2 Model Tuning

The different loading conditions as described in section 3 are evaluated by simulation. In the present study, the empty, the fixed-only and the w/o-trolley loading conditions are investigated.

### 4.2.1 Empty Galley

The comparison of the simulation and test results is shown in Fig. 5. The differences between the dynamic behavior of the starting model in test and simulation can be explained by the non-appropriate support stiffness of the starting model.

Originally the compliance of the aircraft's cabin primary supporting structure was incorporated into the model of the manufacturer using bending support stiffness elements (CELAS-elements). For the tests, carried out at the TUHH's Hexapod test rig as described in section 3, these have to be adapted. Furthermore, the tie rod fastening of the galley to the aircraft primary structure puts a relevant amount of free play into the system. To match the support conditions of the test rig, the support stiffness in the FE-model has to be increased according to the mechanical properties of the supporting test brackets. For the new support condition, the previous CELAS-Elements were replaced with CBUSH-elements. This enables the consideration of the influence of the stiffness in all 6 DoF individually. Especially the introduction of a rotational stiffness to the system's support elements enables a more realistic global dynamic model.

Consequently, by increasing the stiffness

of the support elements, the empty galley model could be tuned to result in a good match between test and simulation results.

The damping of the dynamic system is considered as structural damping (param, G) for all simulation results determined by modal parameter estimation on the basis of the test results.

Both amplification and resonance frequency are closer to the test data and deliver a good prediction of the test results. The mismatch of the resonance frequency and amplification could be reduced to less than 5% in the global mode acceleration transmissibility. Even the interface loads can be modelled more accurately with a maximum difference of a factor of 1,3. Although quantitatively the y-z force curve overestimates the resulting maximum difference by 4 kN, an approximation of the system's dynamic behavior is possible.

Thus, the simple static galley seems accurate enough to predict such a global vibration behavior for the empty loading condition. However, it has to be noted that the model has a high sensitivity to the applied stiffness of the supporting structure.

### 4.2.2 Fixed-only galley loading

During the flight, the galley is usually loaded with different kinds of components, e.g. ovens,

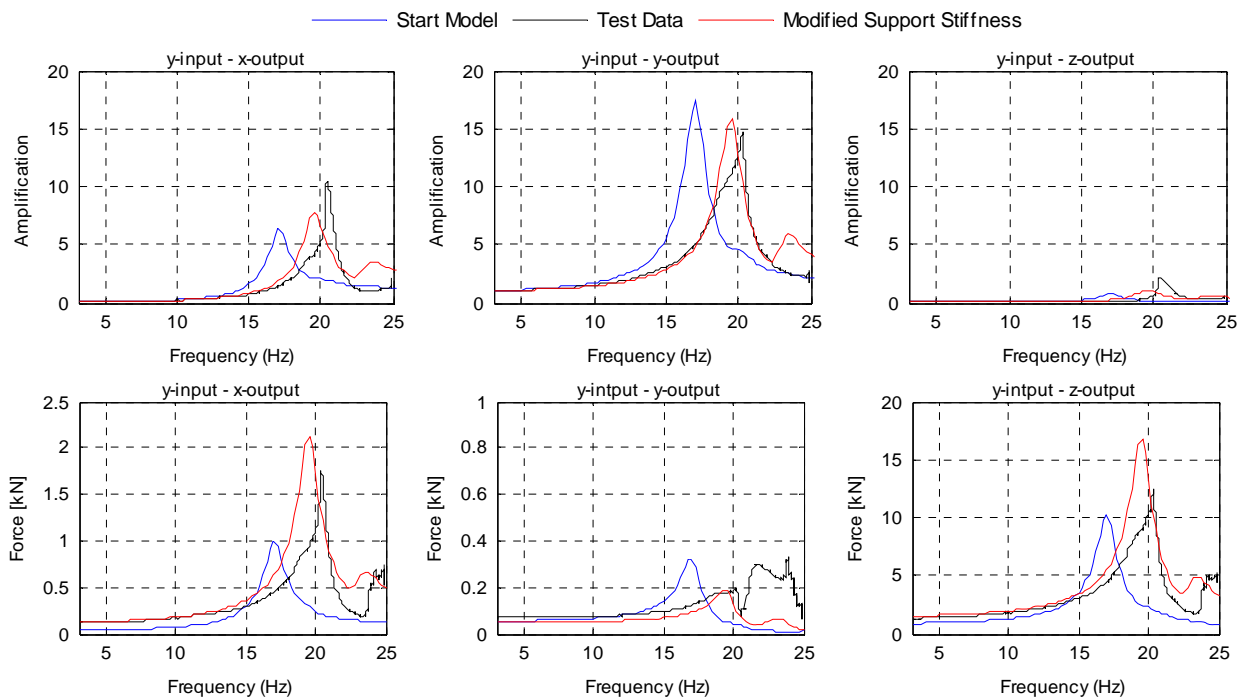


Fig. 6: Simulation results for the 'empty' loading condition – Maximum amplification behavior from y-excitation and resulting hardpoint forces in the frequency range 3 - 25 Hz of hardpoint no. 4

beverage makers or standard units (see Tab.1). These different loading conditions have to be regarded as mechanically different dimensioning cases. Simulations can provide a reasonable forecast of the most critical load case. For the FE-modelling of the additional loading conditions the authors followed up a lumped mass approach (Fig. 7a) as well as a simplified shell modelling of the additional elements. The loadings were implemented as point masses and hollow shell objects (Fig. 7b) that are coupled to the galley structure via interpolation constraint elements.

The test results of this loading condition (Fig. 6) show a different resonance behavior in comparison with the previous results of the empty galley loading. The amplification is significantly lower by a factor of  $\sim 3$ . As described in section 3, the structural damping increases due to the galley loading. In total, all additional masses add up to 96 kg in the “fixed-only” condition.

As expected, the resonance frequency is shifted to a lower frequency. First of all, this is due to the mass increase and the resulting increase of structural damping. The increase in structural damping can be seen by comparing the test results’ different magnitudes over all tests.

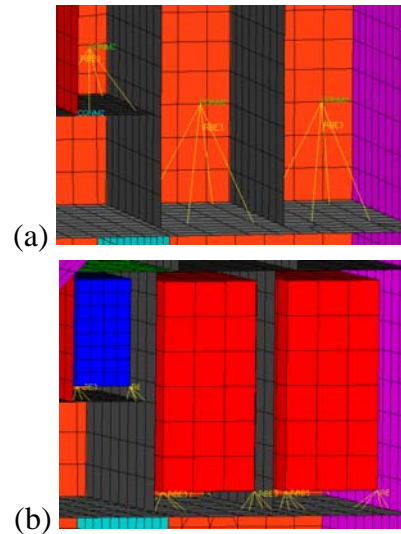


Fig. 8: FE-modelling of different loading conditions with (a) point masses and (b) hollow shell objects of equivalent total mass connected via RBE3-Elements

The test results of the same model as in the empty loading case already provide a reasonable prediction of the resonance behavior regarding the amplification factor as shown in Fig. 6 for the ‘tuned empty model’. However, the resonance frequency appears to be too low if compared to the test results.

Hence, the first approach to fit the simulation to the test results has been reducing the lumped mass. A mass reduction of 20% according to the decoupling of the dynamic

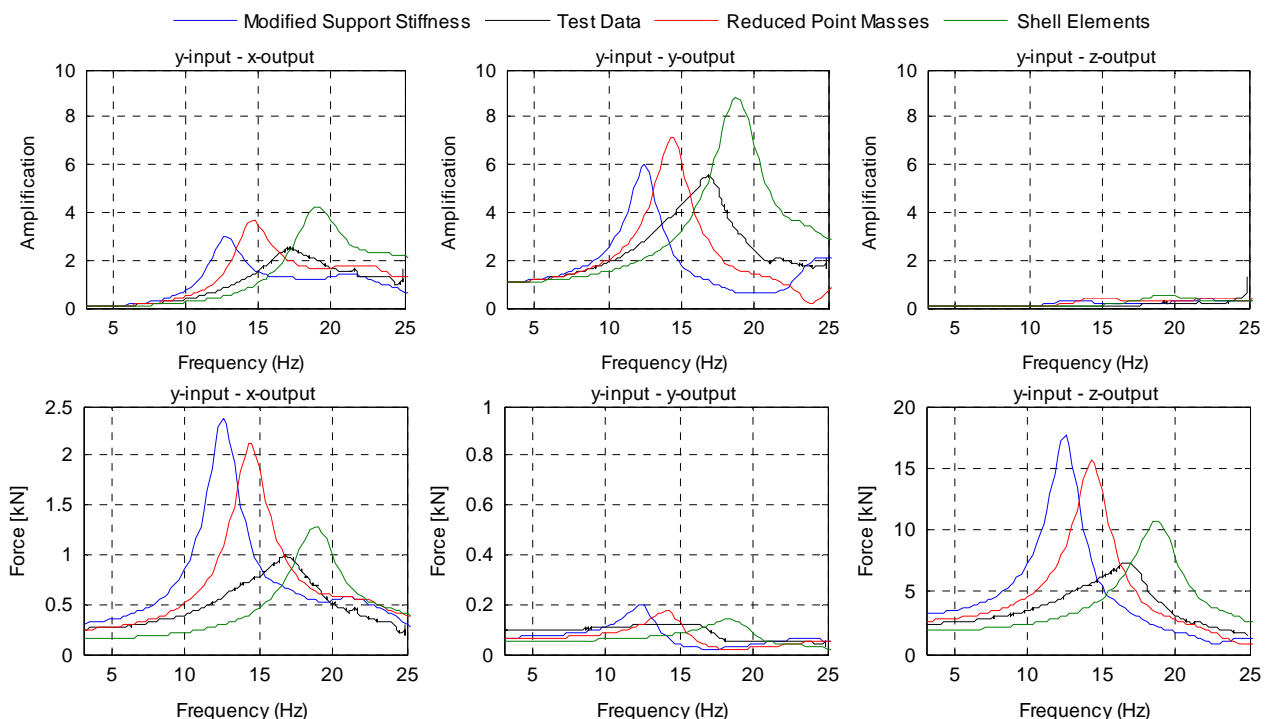


Fig. 7: Simulation results for the ‘fixed-only’ loading condition – Maximum amplification behavior from y-excitation and resulting hardpoint forces in the frequency range 3 - 25 Hz of hardpoint no. 4

mass has led to the results shown in Fig. 6. Furthermore, a certain mass decoupling is assumed because of the loose oven fastening which also reduces the modal effective mass [10]. This leads to a better representation of the test results, but still leaves optimization potential. Therefore, the shell modelling of the galley inserts is presented. The results provide a better representation, especially in terms of the dynamic interface loads. The amplification behavior of the two approaches is of similar accuracy. The predicted peak forces, however, of the model with shell inserts are in a maximum range within 3 kN, whereas the reduced mass model overestimates the interface load by more than a factor of 2. The inertia of the added galley inserts plays an important role and in this case it is possible to predict interface loads more precisely than with the lumped mass approach.

Other lumped mass models were set up for this study, including a connection of the masses via spring-elements. However, these models did not provide reasonable results.

#### 4.2.3 W/O-trolley loading

In order to further validate the presented dynamic modelling approaches, a third loading case is considered. In this case, additional

loading is added as described in Tab.1 for the without-trolley (w/o) loading condition. There are no changes in the model if compared to the previous fixed-only model except for the different loading condition. In case of the w/o trolley condition, the comparison of experimental and simulation results for both introduced approaches shows a similar dynamic response behavior (Fig. 8).

Both modelling approaches represent a good approximation of the resonance behavior with a similar accuracy. The approach that considers the modal effective mass by reducing the added point masses has a slightly lower resonance frequency in the most critical Y-Y-case. Nonetheless, the interface loads match the test results in both cases in contrast to the previous loading conditions. A reason for this result can be the system's higher damping properties as more inserts are placed in the galley as also shown in section 3. More energy seems to dissipate due to loose coupling in the interfaces, which generally reduces magnitude of the interface loads (see also Tab. 2).

### 5 Conclusion and Outlook

In the present study, it could be shown that the simplified state of the art linear static FE-

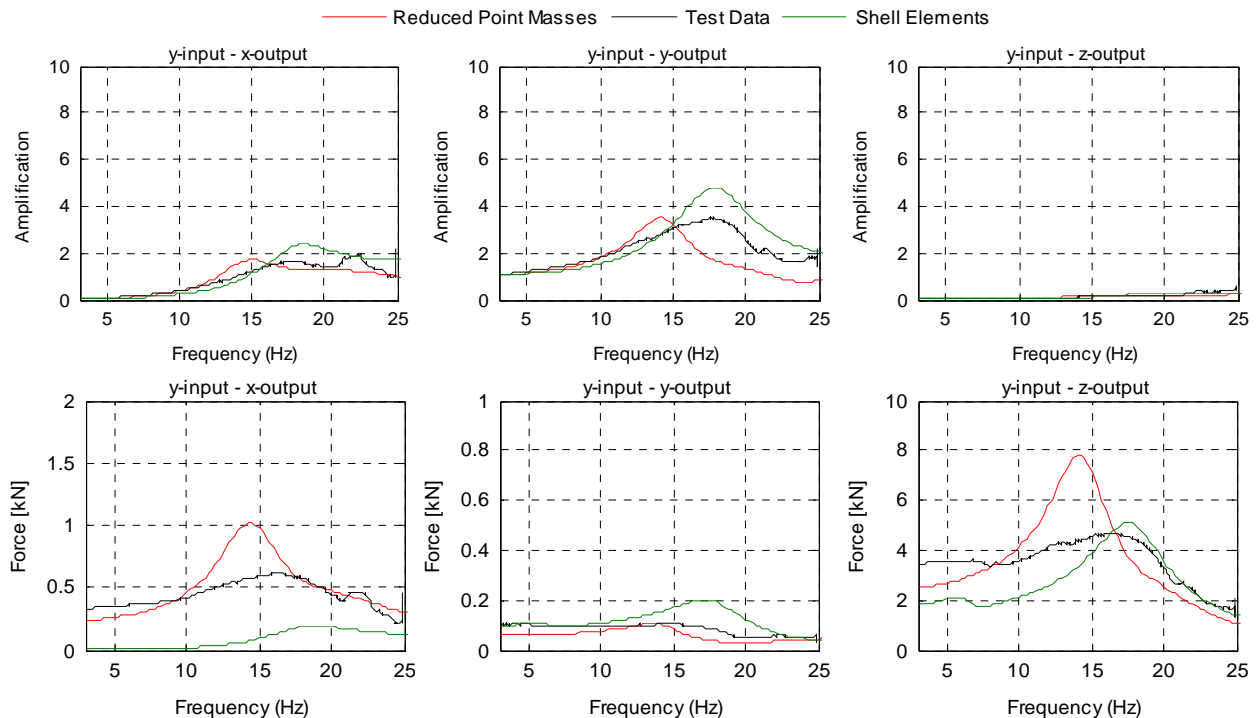


Fig. 9: Simulation results for the 'fixed-only' loading condition – Maximum amplification behavior from y-excitation and resulting hardpoint forces in the frequency range 3 - 25 Hz of hardpoint no. 4

models of large and complex cabin interior monuments can be successfully applied to determine the interface loads and global deflection for stationary dynamic load cases as well. The model tuning benefits from the used Hexapod test facility that enables modal parameter estimation of large and heavy test specimens like galleys in complicated MIMO tests. Two modelling approaches have been presented.

Four main conclusions can be drawn from the present study.

- ➔ The stiffness of the supporting structure significantly influences the dynamic response of the simulation model (especially with regards to the resonance frequency). Therefore, the respective stiffness parameters in the FE-model should be defined with care.
- ➔ Stationary dynamic FE-simulations require an appropriate consideration of damping. For the investigated galley under low frequency excitation, this can be achieved using a global structural damping. The needed model parameter can be derived from experimental results.
- ➔ Various non-linear effects make it generally difficult to model the additional masses of the galley loading under dynamic excitation using a linear numerical model. For example, it could be shown that occurring mass decoupling influences the system's global dynamic behavior.
- ➔ The inertia and the stiffness of the galley inserts have a strong influence on the dynamic behavior of the galley. It seems important to approximate the geometrical dimensions of additional elements in order to predict the amplification behavior as well as interface loads.

The presented approaches to model stationary dynamic loads using a simple linear FE-model seem promising. The simulation models may enable a reduced testing effort of expensive certification tests and facilitate structural optimization. In order to further validate it and to decide which approach is favorable, additional experimental data of other cabin components is currently being analyzed and will be added to the present study in the future.

## References

- [1] Gallardo V et al. *Blade Loss Transient Dynamics Analysis*, NASA-CR-165373-Vol-1 Cincinnati, 1981.
- [2] Wohlgenuth M, et al. Notwendigkeit von detaillierten FE-Modellen zur Effizienzsteigerung der Produktion von Flugzeugküchen, *Proc. 24th DfX-Symp.*, Hamburg, pp. 221-230 (in German), 2013.
- [3] Federal Aviation Administration, AC25-24, 2000.
- [4] European Aviation Safety Agency, CS25, 2012.
- [5] Australian Transport Safety Bureau, Examination of a Failed Fan Blade Turbofan Engine, Investigation Number 200100445, 2001.
- [6] Aviation Rulemaking Advisory Committee, Engine Windmilling Imbalance Loads - Final Report -, 1997.
- [7] Bureau of Transportation Statistics (BTS), 2013.
- [8] General Aviation Manufacturers Association, Acceptable Practices Document, Cabin Interior Monument Structural Substantiation Methods, 2009.
- [9] Plaumann B and Krause D A methodical approach for dynamic system analysis & synthesis in the dimensioning of variant lightweight cabin interior. *Proc. ICAS 2014*, St. Petersburg, 2014.
- [10] Girard A and Roy N *Structural Dynamics in Industry*. Wiley-VCH, 2007.
- [11] Avitable P, et al. Modal Parameter Estimation for Large, Complicated MIMO Tests, *J. o. Sound and Vibration*, Vol. 40, No. 1, pp14-20, 2006.
- [12] Plaumann B et al. Dynamic simulation and testing for lighter cabin interior. *Proc. 4th International Workshop on Aircraft System Technologies (AST)*, Hamburg, pp. 211-220, 2013.
- [13] Plaumann B, et al. System analysis and synthesis for the dimensioning of variant lightweight cabin interior. *Proc. 54th AIAA/ASME/ASCE/AHS/ASC Struct., Struct. Dyn. a Mat. Conf.*, Boston 2013.

## Contact Author Email Address

[j.oltmann@tuhh.de](mailto:j.oltmann@tuhh.de)

The authors would like to thank the Federal Ministry of Economic Affairs and Energy for funding the research project "simoUNITS" and the cooperation partner Diehl Service Modules GmbH for providing test specimens and valuable application background.

## Copyright Statement

The authors confirm that they and/or their company or organization, hold copyright on all of the original material included in this paper. The authors also confirm that they have obtained permission, from the copyright holder of any third party material included in this paper, to publish it as part of their paper. The authors confirm that they give permission, or have obtained permission from the copyright holder of this paper for the publication and distribution of this paper as part of the ICAS 2014 proceedings or as individual off-prints from the proceedings.